Cell and Tissue Research (2021) 385:539–555
https://doi.org/10.1007/s00441-021-03438-3

REGULAR ARTICLE

Temporal dynamics of cells expressing NG2 and platelet-derived growth factor receptor-β in the fibrotic scar formation after 3-nitropropionic acid-induced acute brain injury

Tae-Ryong Riew[1] · Xuyan Jin[1,2] · Soojin Kim[1] · Hong Lim Kim[3] · Mun-Yong Lee[1,2]

Received: 29 October 2020 / Accepted: 18 February 2021 / Published online: 17 April 2021

Abstract

Neuron-glia antigen 2 (NG2) proteoglycan and platelet-derived growth factor receptor beta (PDGFR-β) are widely used markers of pericytes, which are considered cells that form fibrotic scars in response to central nervous system insults. However, the exact phenotypes of NG2- and PDGFR-β-expressing cells, as well as the origin of the fibrotic scar after central nervous system insults, are still elusive. In the present study, we directly examined the identities and distributions of NG2- and PDGFR-β-positive cells in the control and lesioned striatum injured by the mitochondrial toxin 3-nitropropionic acid. Immunoelectron microscopy and correlative light and electron microscopy clearly distinguished NG2 and PDGFR-β expression in the vasculature during the post-injury period. Vascular smooth muscle cells and pericytes expressed NG2, which was prominently increased after the injury. NG2 expression was restricted to these vascular mural cells until 14 days post-lesion. By contrast, PDGFR-β-positive cells were perivascular fibroblasts located abluminal to smooth muscle cells or pericytes. These PDGFR-β-expressing cells formed extravascular networks associated with collagen fibrils at 14 days post-lesion. We also found that in the injured striatal parenchyma, PDGFR-β could be used as a complementary marker of resting and reactive NG2 glia because activated microglia/macrophages shared only the NG2 expression with NG2 glia in the lesioned striatum. These data indicate that NG2 and PDGFR-β label different vascular mural and parenchymal cells in the healthy and injured brain, suggesting that fibrotic scar-forming cells most likely originate in PDGFR-β-positive perivascular fibroblasts rather than in NG2-positive pericytes.

Keywords 3-Nitropropionic acid · Perivascular adventitial cell · Fibrotic scar · PDGFR-β · NG2 glia

Introduction

Insults to the central nervous system (CNS) trigger the formation of glial and fibrotic scars (Fernandez-Klett and Priller 2014). Fibrotic scars are generally known to impede axonal regeneration, thus hindering functional recovery after CNS insults, although other studies suggest they could function as a physical barrier that restricts inflammatory processes, promoting tissue remodeling (Cha et al. 2014; Yoshioka et al. 2010; Zhu et al. 2015). Despite the increasing awareness of the functional implications of fibrotic scars, the precise identity of scar-forming cells after CNS insults has long been debated. Goritz et al. reported that type A pericytes expressing platelet-derived growth factor receptor beta (PDGFR-β) detach from blood vessels and differentiate into fibrotic scar-forming cells after spinal cord injury (Goritz et al. 2011). On the other hand, other studies reported that perivascular stromal cells or perivascular fibroblasts that express PDGFR-β yet are distinct from pericytes are accountable for fibrotic scar formation (Fernandez-Klett et al. 2013; Soderblom et al. 2013). In support of this, we have previously demonstrated that perivascular adventitial fibroblasts expressing PDGFR-β do not fit the classical definition of pericytes and contribute to fibrotic scar formation after acute brain injury (Riew et al. 2018).

✉ Mun-Yong Lee
munylee@catholic.ac.kr

[1] Department of Anatomy, Catholic Neuroscience Institute, College of Medicine, The Catholic University of Korea, Seoul 06591, Republic of Korea

[2] Department of Biomedicine and Health Sciences, College of Medicine, The Catholic University of Korea, Seoul 06591, Republic of Korea

[3] Integrative Research Support Center, Laboratory of Electron Microscope, College of Medicine, The Catholic University of Korea, Seoul 06591, Republic of Korea

In addition to PDGFR-β-positive cells, cells expressing neuron-glia antigen 2 (NG2) have been proposed as an alternative source of fibrotic scarring following CNS insults. Hesp et al. reported that dividing NG2-positive pericytes are necessary for intralesional angiogenesis and fibrotic scar formation after spinal cord injury (Hesp et al. 2018). Additionally, NG2 glia, a distinct class of glial cells in the CNS, undergo dynamic changes, forming a dense network in the fibrotic scar-forming area after brain insults (Jin et al. 2018). Taken together, three types of cells, NG2 glia, NG2-positive pericytes, and PDGFR-β-positive fibroblast-like cells, are deemed key players in the fibrotic scar formation in response to CNS insults.

From the perspective of specific marker expression in the CNS vasculature, NG2 and PDGFR-β are widely accepted as markers of pericytes (Armulik et al. 2011; Krueger and Bechmann 2010; Lindahl et al. 1997; Schultz et al. 2017; Smyth, et al. 2018; Winkler et al. 2010). However, NG2 proteoglycan is expressed in a wide range of other cell types including vascular mural cells and NG2 glia in the adult brain, and NG2 is also induced in activated microglia/macrophages (Dimou and Gallo 2015; Jin et al. 2018, 2020; Nishiyama et al. 1997; Ozerdem et al. 2001). In addition, PDGFR-β expression is found in NG2 glia and astrocytes in the epileptic brain (Kyyriainen et al. 2017). Despite abundant information about the heterogeneous populations of NG2- and PDGFR-β-positive cells in both control and the injured brain, direct comparisons of their distribution and morphology remain to be established.

In the present study, we compared the distribution and morphological features of cells expressing NG2 and PDGFR-β at the regional, cellular, and subcellular levels in the lesioned striatum following injection of the natural mitochondrial toxin 3-nitropropionic acid (3-NP). This toxin produces a well-demarcated lesion core, where all types of cells exhibit pan-necrosis, and a resultant fibrotic scar forms (Duran-Vilaregut et al. 2010; Jin et al. 2018; Mu et al. 2016; Riew et al. 2017). We focused our attention on the spatiotemporal distribution of two markers associated with vessels in the development of the fibrotic scar after 3-NP injection. Vascular mural cells reside in close proximity within the perivascular space, and there are no perfect markers to distinguish between these cells with light microscopy. Therefore, we combined an immunoperoxidase method with a correlative light and electron microscopy (CLEM) approach to identify the exact phenotype of vessel-associated NG2- and PDGFR-β-expressing cells.

Material and methods

Animal preparation

All procedures and provisions for animal care were in accordance with the Laboratory Animals Welfare Act, the Guide for the Care and Use of Laboratory Animals, and the Guidelines and Policies for Rodent Survival Surgery provided by the IACUC (Institutional Animal Care and Use Committee) at the College of Medicine of The Catholic University of Korea (approval number CUMS-2020-0041-01). IACUC and the Department of Laboratory Animals in the Catholic University of Korea, Songeui Campus, accredited the Korea Excellence Animal Laboratory Facility from the Korea Food and Drug Administration in 2017 and acquired full Association for Assessment and Accreditation of Laboratory Animal Care International accreditation in 2018. All efforts were made to minimize animal suffering and to reduce the number of animals used.

Twenty-five adult male Sprague-Dawley rats (250–300 g; OrientBio, Seongnam, Republic of Korea) were used for light- and electron-microscopic studies. The animals were housed in groups of three per cage in a controlled environment at a constant temperature (22 ± 5 °C) and humidity (50 ± 10%) with food (gamma ray-sterilized diet) and water (autoclaved tap water) available ad libitum. The rats were maintained on a 12-h light/dark cycle. The mitochondrial toxin 3-NP (Sigma-Aldrich, St. Louis, MO, USA) was dissolved in buffered saline (pH = 7.0) and administered intraperitoneally (i.p.) at a dose of 15 mg/kg once daily for 3 days. Only rats exhibiting behavioral deficits such as hindlimb impairment or kyphotic posture, recumbency, or impaired postural adjustment were included in the experimental group (Hamilton and Gould 1987). Animals were euthanized 3, 7, and 14 days after the final injection of 3-NP ($n = 5$ rats per time point). The control group ($n = 4$) received i.p. injections of the same volume of normal saline for three consecutive days. The rats in this group were euthanized 3 days after the final injection. After anesthesia with zolazepam (20 mg/kg i.p.) and xylazine (7.5 mg/kg i.p.), the animals were transcardially perfused with 4% paraformaldehyde in 0.1 M phosphate buffer (PB, pH 7.4) for light or electron microscopy. The brain tissues were equilibrated with 30% sucrose in 0.1 M PB, frozen, and stored at − 70 °C for light microscope studies.

Immunohistochemistry

For double or triple immunofluorescence immunohistochemistry, free-floating sections (25 μm thick) were blocked in blocking buffer (a mixture of 0.2% gelatin, 1% bovine serum albumin, and 0.05% saponin or a mixture of 10% normal serum, 1% bovine serum albumin, and 0.1% triton), then incubated at 4 °C overnight with a mix of primary antibodies. Primary antibodies and dilutions were as follows: mouse anti-NG2 (1:200; Millipore, Temecula, CA, USA), rabbit anti-NG2 (1: 200, Millipore), rabbit anti-PDGFR-β (1:200; Abcam, Cambridge, UK), rabbit

anti-CD13 (1:300; Abcam), goat anti-ionized calcium-binding adaptor molecule 1 (Iba1; 1:500; Abcam), mouse anti-rat endothelial cell antigen-1 (RECA1; 1:200; Bio-Rad, Hercules, CA, USA), and goat anti-type IV collagen (1:100; Bio-Rad). In some experiments, double-labeling was performed using a mixture of mouse anti-adenomatous polyposis coli (APC; also called CC1; 1:100; Sigma-Aldrich) and either rabbit anti-NG2 (1: 200, Millipore) or rabbit anti-PDGFR-β (1:200; Abcam). Some sections were also incubated with a mixture of goat anti-type IV collagen (1:100; Bio-Rad) and rabbit anti-collagen I (1:200, Abcam). This triple- or double-labeling was followed by a 2-h incubation with appropriate secondary antibodies, as follows: Cy3-conjugated goat anti-mouse antibody (1:2000; Jackson ImmunoResearch, West Grove, PA, USA), Cy3-conjugated goat anti-rabbit antibody (1:2000; Jackson ImmunoResearch), Cy3-conjugated donkey anti-goat antibody (1:2000; Jackson ImmunoResearch), Alexa Fluor 488-tagged goat anti-rabbit antibody (1:300; Thermo Fisher, Waltham, MA, USA), Alexa Fluor 488-tagged goat anti-mouse antibody (1:300; Thermo Fisher), Alexa Fluor 488-tagged donkey anti-mouse antibody (1:300; Thermo Fisher), or Alexa Fluor 647-tagged donkey anti-rabbit antibody (1:300; Thermo Fisher). Counterstaining of cell nuclei was carried out with 4′, 6-diamidino2′-phenylindole (DAPI; 1:2000; Roche, Mannheim, Germany) for 10 min. For negative staining the controls for double- or triple-labeling, each primary antibody was omitted before sections were incubated with the corresponding secondary antibody. In addition, we compared the results of triple-labeling with those of single- and double-labeling for all combinations of antibodies to yield clearly interpretable data and avoid cross reactivity. Slides were viewed under a confocal microscope (LSM800 with Airyscan; Carl Zeiss Co., Ltd., Oberkochen, Germany) equipped with four lasers (Diode 405, Argon 488, HeNe 555, and HeNe 639) under constant viewing conditions. Fluorescence intensity profiles were obtained using Zen 2.3 blue edition (Carl Zeiss Co., Ltd.). For three-dimensional (3D) reconstruction, NG2 and PDGFR-β signals were 3D-rendered using IMARIS (Bitplane, Switzerland).

For quantitative analysis, confocal images were obtained with a 40×objective lens with constant viewing settings. Mean NG2 or PDGFR-β intensity outside RECA-1 expressing blood vessels was measured from a randomly selected area (24 × 24 µm) in 9.5-µm maximal intensity z-projection. Three images were obtained per animal, and in each image, three to six areas were selected for analysis. To compare the number of Iba1-positive activated microglia and NG2 glia, we used 160 × 160 µm images of 6 µm Z-stacks with 0.5-µm optical sections, only counting cells with cytoplasmic expression of each molecule encircling nuclei. The number of animals used for each analysis is indicated in the figure legends of Figs. 2 and 6.

Immunoelectron microscopy

For pre-embedding immunoelectron microscopy, semi-thin cryosections (2 µm thick) or floating vibratome sections (50 µm thick) were made from control and experimental rats ($n = 3$ rats per time point) at 3 and 14 days after 3-NP injection. Semi-thin cryosections were cut at − 100 °C with a glass knife in a Leica EM UC7 ultramicrotome equipped with an FC7 cryochamber (Leica, Wetzlar, Germany). The sections were blocked with 10% normal goat serum and 1% bovine serum albumin in 0.01 M phosphate buffered saline for 1 h and then immunostained with rabbit anti-NG2 (1:200, Millipore), rabbit anti-PDGFR-β (1:200; Abcam), or rabbit anti-CD13 (1:100; Abcam) overnight at 4 °C. Primary antibodies were visualized using peroxidase-conjugated goat anti-rabbit IgG (1:100; Jackson Immunoresearch) and 0.05% 3,3′-diaminobenzidine tetrahydrochloride (DAB) with 0.01% H_2O_2 as the substrate. After fixation, dehydration, and embedding in Epon 812 (Polysciences, Warrington, PA, USA), areas of interest were excised and glued onto resin blocks. Ultrathin sections (70 nm thick) were cut, stained with 2% uranyl acetate for 10 min, and observed under an electron microscope (JEM 1010, JEOL, Tokyo, Japan).

To analyze the expression of NG2 or PDGFR-β in the pericytes of capillaries, electron micrographs of 7–10 randomly selected capillaries were obtained from three rats per group, which corresponds to approximately 20–30 capillaries per sham-operated or experimental rat, at days 3 and 14 after 3-NP injection. Only cross-sectioned capillaries that were covered by pericytes and showed typical morphological features—i.e., having processes that extend around the capillary wall and are completely bounded by a basal lamina—were included in the analysis (Attwell et al. 2016; Krueger and Bechmann 2010).

For CLEM, semi-thin cryosections (2 µm thick) were double-labeled at 4 °C overnight using mouse monoclonal antibody against NG2 (1:200; Millipore) and rabbit polyclonal antibody against PDGFR-β (1:200; Abcam). Antibody staining was visualized using Cy3-conjugated goat anti-mouse antibody (1:2000; Jackson ImmunoResearch) and Alexa Fluor 488-tagged goat anti-rabbit antibody (1:300; Thermo Fisher). Sections were labeled with DAPI for 10 min. Coverslipped sections were examined with a confocal microscope and photographed at various magnifications with a differential interference contrast setting to find specific areas for later examination by electron microscopy. After the coverslips had been floated off the sections, the tissues were prepared further for electron microscopy, as described above.

Statistics

Statistical significance was determined by one-way analysis of variance (ANOVA) followed by Tukey's multiple comparisons

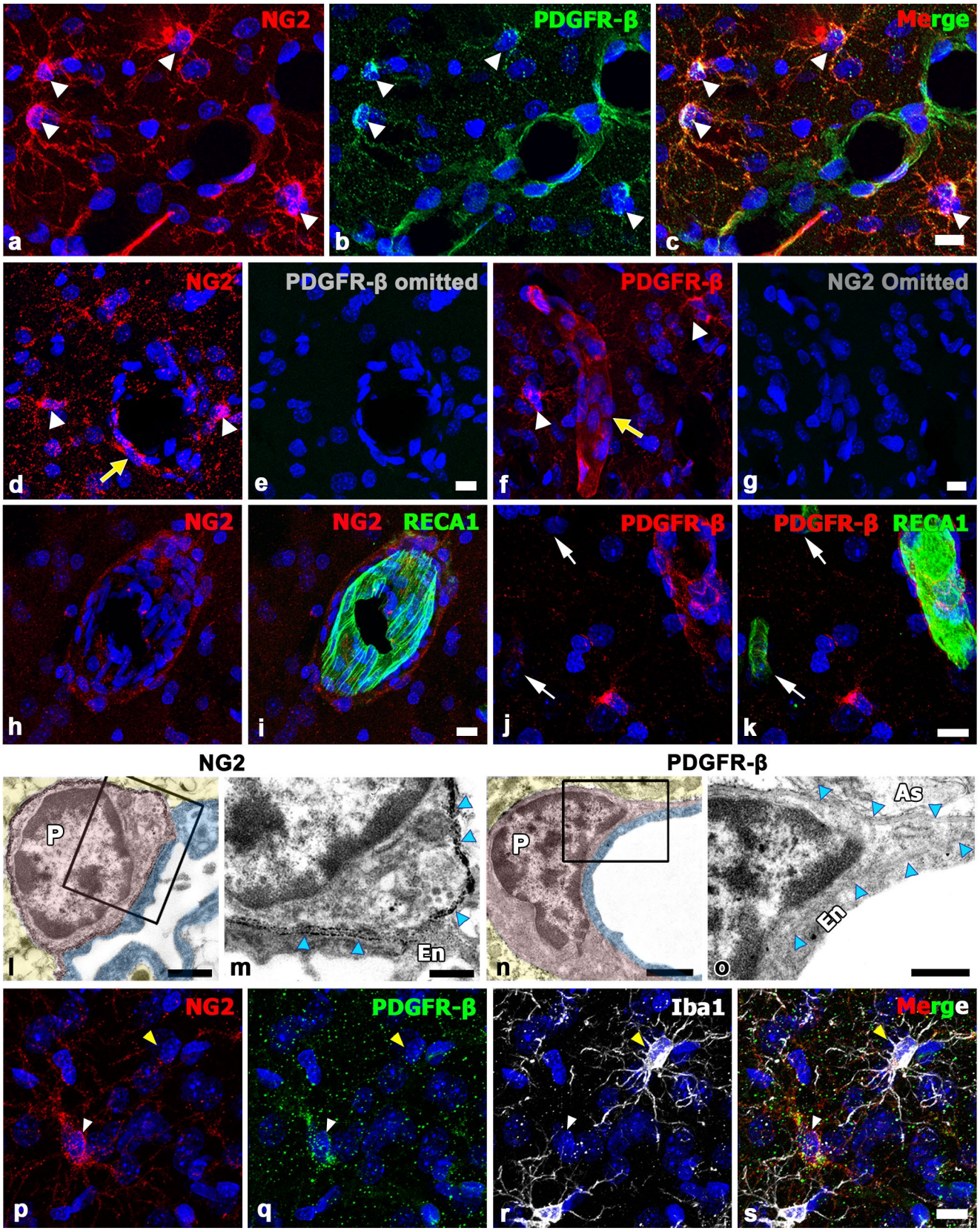
NG2
PDGFR-β
Merge
a
b
c
NG2
PDGFR-β omitted
PDGFR-β
NG2 Omitted
d
e
f
g
NG2
NG2 RECA1
PDGFR-β
PDGFR-β RECA1
h
i
j
k
NG2
PDGFR-β
P
En
P
As
En
l
m
n
o
NG2
PDGFR-β
Iba1
Merge
p
q
r
s

◂**Fig. 1** Cellular localization of neuron-glia antigen 2 (NG2) and platelet-derived growth factor receptor beta (PDGFR-β) and their relationship in the striatum of saline-treated control rats. **a–c** Representative images of double-labeling for NG2 and PDGFR-β show that both signals are observed within vascular profiles and surrounding extravascular areas. Note that vascular NG2 expression is very weak, while vessel-associated PDGFR-β is more prominent. Moreover, note that parenchymal cells with fine processes (arrowheads) co-express NG2 and PDGFR-β. Negative controls for the double-labeling performed by omitting PDGFR-β **d, e** or NG2 **f, g** and subsequently incubating them with the corresponding secondary antibody show the absence of specific immunoreactivity to PDGFR-β or NG2. Arrows indicate vessel-associated cells, and arrowheads indicate parenchymal cells. **h–k** Double-labeling for the vascular endothelial cell marker rat endothelial cell antigen-1 (RECA1) and either NG2 or PDGFR-β. Note that very weak NG2 expression can be detected along the outer part of vascular endothelial cells. Further, note that PDGFR-β is localized in vessels of a larger caliber but is absent in capillary-like microvessels (arrows). **l–o** Comparison of NG2- and PDGFR-β-positive cells associated with capillaries in the control striatum using alternatively performed pre-embedding immunoelectron microscopy. **l**, **m** NG2 is specifically localized along the plasma membrane (arrowheads in m) of the pericytes (P; shaded in red) of capillaries, which are closely apposed to endothelial cells (En; shaded in blue). The boxed area in **l** is enlarged in **m**. Note that endothelial cells are devoid of NG2. **n**, **o** No specific PDGFR- β immunoreactivity can be detected in either the endothelial cells (En; blue) or pericytes (P; red) of capillaries. The boxed area in **n** is enlarged in **o**. Note that the basal lamina (arrowheads in **o**) surrounding the pericytes is in direct contract with the glia limitans (As; shaded in yellow). Data are representative of 20 capillaries from three rats. **p–s** Triple-labeling for NG2. PDGFR-β, and the microglial marker ionized calcium-binding adaptor molecule 1 (Iba1) shows that NG2/PDGFR-β double-labeled cells (white arrowheads), presumptively NG2 glia, are distinct from resting microglia (yellow arrowheads). Light microscopy data from three rats are presented. Cell nuclei appear blue after 4′,6-diamidino-2′-phenylindole (DAPI) staining. Scale bars = 10 μm for **a–k, p-s**; 1 μm for **l, n**; 0.5 μm for **m, o**

test. Differences with $p < 0.05$ were considered significant. All statistical calculations were performed using GraphPad Prism version 8 (GraphPad Software Inc., San Diego, CA, USA).

Results

Consistent with our previous data, about 70% of the rats intoxicated with 3-NP in the present study developed the characteristic neurological deficits including hindlimb impairment, recumbency, and impaired postural adjustment (Choi et al. 2017; Jin et al. 2018; Riew et al. 2017).

Cellular localization of and relationship between NG2 and PDGFR-β in the control striatum

We first analyzed the expression of and relationship between NG2 and PDGFR-β in the striatum of saline-treated control rats. Both NG2 and PDGFR-β were observed within vascular profiles, where NG2 immunoreactivity was very weak, but PDGFR-β expression was more prominent (Fig. 1a–c). Both signals were also observed in parenchymal cells with ramified processes (Fig. 1a–c), which were most likely NG2 glia based on their morphology and the co-expression of both markers (Kyyriainen et al. 2017; Riew et al. 2018). Immunoreactivity specific to NG2 or PDGFR-β was eliminated when the omission of each primary antibody and subsequent incubation of corresponding secondary antibody was performed (Fig. 1d–g). In addition, the comparison of the double-labeling (Fig. 1a–c) and the single labeling for NG2 or PDGFR-β (Fig. 1d–g) did not yield any differences in the localization of the two molecules.

We further investigated the association between the two markers and blood vessels using the vascular endothelial cell marker RECA1. Vascular NG2 expression was detected along the outer part of vascular endothelial cells (Fig. 1h, i). As shown in Fig. 1j, k, PDGFR-β expression was localized in vessels of a larger caliber but was absent in capillary-like microvessels. Using alternatively performed pre-embedding immunoelectron microscopy, we investigated the cellular identity of vascular cells expressing NG2 and PDGFR-β in the control striatum. NG2 immunoreactivity, as indicated by highly electron-dense DAB grains, was specifically associated with the plasma membrane of the pericytes of capillaries (Fig. 1l, m). As reported previously (Riew et al. 2018), PDGFR-β immunoreactivity was not detected in the pericytes of capillaries (Fig. 1n, o). We found that all of pericytes in each of the 20 capillaries analyzed were positive for NG2 but negative for PDGFR-β. Both NG2 and PDGFR-β were not detected in the endothelial cells of capillaries (Fig. 1l–o). Next, we performed double-labeling using the pericyte marker CD13 (Armulik et al. 2010) and RECA1. As shown in Supplementary Fig. 1a–c, CD13 expression was closely in contact with vasscular endothelial cells. In addition, pre-embedding immunoelectron microscopy showed CD13 immunoreactivity in the pericytes (Supplementary Figs. 1d, e).

In addition, triple-labeling for NG2, PDGFR-β, and the microglial marker Iba1 revealed that NG2/PDGFR-β double-labeled NG2 glia were devoid of Iba1 immunoreactivity (Fig. 1p–s), as reported previously (Garbelli et al. 2015; Jin et al. 2018). Moreover, double-labeling with either NG2 or PDGFR-β, and APC, a marker of mature oligodendrocytes (Casella et al. 2004), revealed the non-overlapping expression of two molecules with APC in the control striatum—despite APC-positive oligodendrocytes being clearly observed (Supplementary Figs. 2a–f).

Spatiotemporal profiles of and relationship between vessel-associated cells expressing NG2 and PDGFR-β in the striatum in the early phase following 3-NP injection

Next, we examined the spatiotemporal distribution of NG2 and PDGFR-β in the rat striatum subjected to 3-NP. Three days after the injury, the lesion core was evident in the

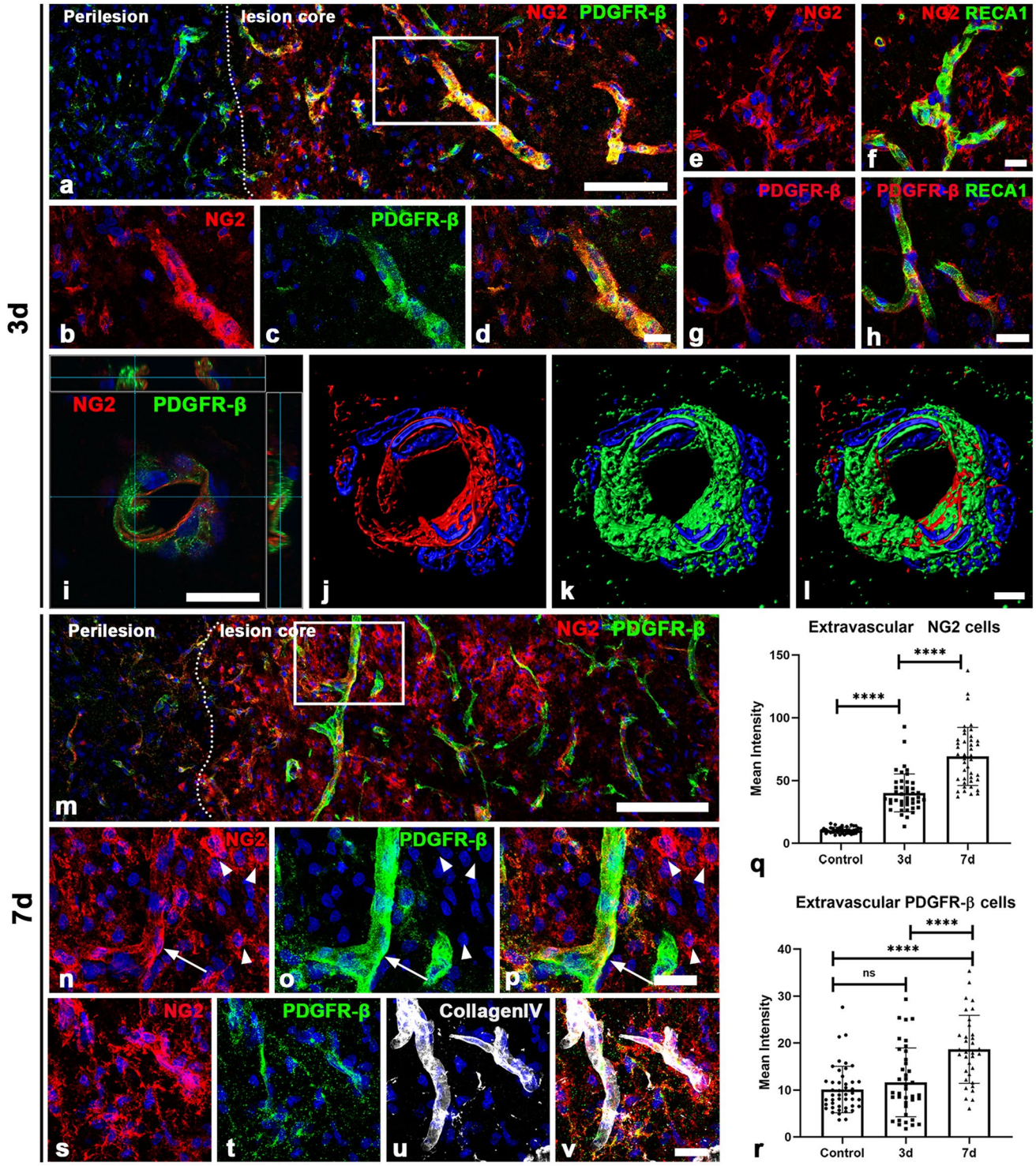

lateral part of the striatum, where astrocytes had virtually disappeared in the lesion core (data not shown), as described previously (Choi et al. 2017; Duran-Vilaregut et al. 2010; Jin et al. 2018; Mu et al. 2016; Riew et al. 2017; Wullner et al. 1994). At this time point, intense PDGFR-β expression was noted in vascular profiles of both the perilesional area and the lesion core, whereas vascular NG2 expression was prominent only in the lesion core (Fig. 2a–d). We further characterized these vascular distributions by double-labeling for RECA1 and either NG2 or PDGFR-β. NG2 expression was localized to vessels and parenchymal cells in the extravascular area (Fig. 2e, f), whereas PDGFR-β was noted preferentially within vessels (Fig. 2g, h). Orthogonal images revealed that PDGFR-β appeared to be localized on

◂**Fig. 2** Spatiotemporal distribution of and relationship between neuron-glia antigen 2 (NG2) and platelet-derived growth factor receptor beta (PDGFR-β) in the lesioned striatum on days 3 and 7 after 3-nitropropionic acid (3-NP) injection. Lower **a** and higher **b–d** magnification views of the striatum 3 days post-lesion. Notably, intense PDGFR-β expression is present within vascular profiles of both the lesion core (to the right of the dotted line) and the perilesional area (perilesion), whereas vascular NG2 expression is prominent only in the lesion core. **e–h** Double-labeling for the vascular endothelial cell marker rat endothelial cell antigen-1 (RECA1) and either NG2 or PDGFR-β shows that NG2 is detectable within vessels and parenchymal cells in the extravascular area, whereas PDGFR-β is noted preferentially within vessels. **i** Orthogonal view, revealing the spatial relationship between PDGFR-β and NG2 within vessels in the lesion core. Note that PDGFR-β appears to be localized on the abluminal side of NG2-positive cells. **j–l** Three-dimensional rendering of the image shown in **i** indicates the different spatial relationship of the two proteins within vessels. Lower **m** and higher **n–p** magnification views of the striatum 7 days post-lesion. Both NG2 and PDGFR-β are noted within vessels (arrows) in the lesion core (to the right of the dotted line). Note that the number of parenchymal NG2-positive cells (arrowheads) that are devoid of PDGFR-β appears to increase in extravascular areas in comparison to the 3-day time point. **q**, **r** Quantitative temporal analysis of the mean fluorescence intensities of NG2 and PDGFR-β expression in extravascular areas over a 7-day period after lesion induction. Note that the relative intensity of both NG2 and PDGFR-β progressively increased at 3–7 days post-lesion. $n = 3$ rats per group. Data are expressed as mean ± SEM. ns, not significant; $^{****}P < 0.0001$; one-way ANOVA followed by Tukey's multiple comparison test. **s–v** Triple-labeling for NG2, PDGFR-β, and collagen IV in the lesion core shows that both proteins are noted in vessels with different expression patterns. Light microscopy data from three rats per group are presented. Cell nuclei appear blue after 4′,6-diamidino-2′-phenylindole (DAPI) staining. Scale bars = 100 µm for **a**, **m**; 20 µm for **b–i**, **n–p, s–v**; 5 µm for **j–l**

the abluminal side of NG2-positive cells within vessels, with these cells being closely associated with each other (Fig. 2i). In addition, the 3D-rendered image revealed their different spatial relationship within vessels (Fig. 2j–l). Seven days after the 3-NP injection, the labeling patterns for NG2 and PDGFR-β in the lesion core were similar to those observed on day 3, but there was a more prominent enrichment of NG2-positive cells in extravascular areas (Fig. 2m–p). Quantitative analysis revealed a significant increase in the mean fluorescence intensities of NG2 and PDGFR-β expression in extravascular areas at 3–7 days post-lesion than in the control (Fig. 2q, r). Triple-labeling for NG2, PDGFR-β, and collagen IV, the principal collagen type in the neurovascular basal lamina, revealed that both NG2 and PDGFR-β were associated with vessels, but they exhibited different patterns within vessels (Fig. 2s–v).

However, light-microscopic imaging alone was not sufficient to clarify the identity of vascular cells expressing these two proteins. Using alternatively performed pre-embedding immunoelectron microscopy, we investigated the ultrastructural morphology of vascular cells expressing NG2 and PDGFR-β. NG2 immunoreactivity, as indicated by highly electron-dense DAB grains, was specifically associated with the plasma membrane and its adjacent extracellular matrix of smooth muscle cells of venules but not with endothelial cells (Fig. 3a, c). In the lesioned striatum of the same experimental animal, however, PDGFR-β-positive cells had long cytoplasmic processes that invariably laid on the abluminal side of smooth muscle cells, which did not express PDGFR-β and often formed a multilayered sheath (Fig. 3b, d, e). They had euchromatic nuclei and well-developed rough endoplasmic reticulum with marked dilation, indicating that they were most likely perivascular fibroblast-like cells, as described previously (Riew et al. 2018). In this regard, PDGFR-β-positive cells seemed to abut the abluminal surface of NG2-positive smooth muscle cells (Fig. 3c, d). In arterioles, electron-dense NG2 staining was also localized along the plasma membranes of smooth muscle cells (Supplementary Fig. 3). On their abluminal side, NG2-negative cells had large euchromatic nuclei with prominent nucleoli and dilated cisternae of rough endoplasmic reticulum (Supplementary Fig. 3), indicating that they corresponded to PDGFR-β-positive fibroblasts.

In capillaries, NG2 expression was localized along the plasma membrane of pericytes but was not detected in adjacent cells that had dilated cisternae of rough endoplasmic reticulum (Fig. 4a, b). In the same striatum, PDGFR-β was detected in long cytoplasmic processes that were located on the abluminal side of endothelial cells and pericytes of capillaries, both of which were negative for PDGFR-β (Fig. 4c, d). These expression patterns of NG2 or PDGFR-β in the pericytes of capillaries were confirmed in at least each of 20 capillaries analyzed. These data indicate that pericytes and smooth muscle cells expressed NG2, whereas PDGFR-β labeled adventitial fibroblast-like cells. To further clarify the cellular identity of vascular NG2- and PDGFR-β-positive cells, we used a CLEM approach. Semi-thin sections double-labeled for NG2 and PDGFR-β were first observed using confocal microscopy, and the same semi-thin sections were subsequently subjected to electron microscopy (Fig. 5a–e). Overlay of the confocal microscopy and transmission electron microscopy data clearly revealed that the PDGFR-β-positive cell in this figure had a large euchromatic nucleus with a prominent nucleolus, well-developed rough endoplasmic reticulum (Fig. 5e, g, h) and was closely abutted to NG2-positive smooth muscle cells (Fig. 5f–h).

Differential expression of NG2 and PDGFR-β in NG2 glia and activated microglia/macrophages

Several reports have provided evidence that NG2 expression is induced in activated microglia/macrophages following CNS insults (Bu et al. 2001; Jin et al. 2018, 2020; Jones et al. 2003; Matsumoto et al. 2008; Zhu et al. 2012). To clarify the phenotypes of parenchymal cells expressing NG2 and PDGFR-β, we performed triple-labeling with

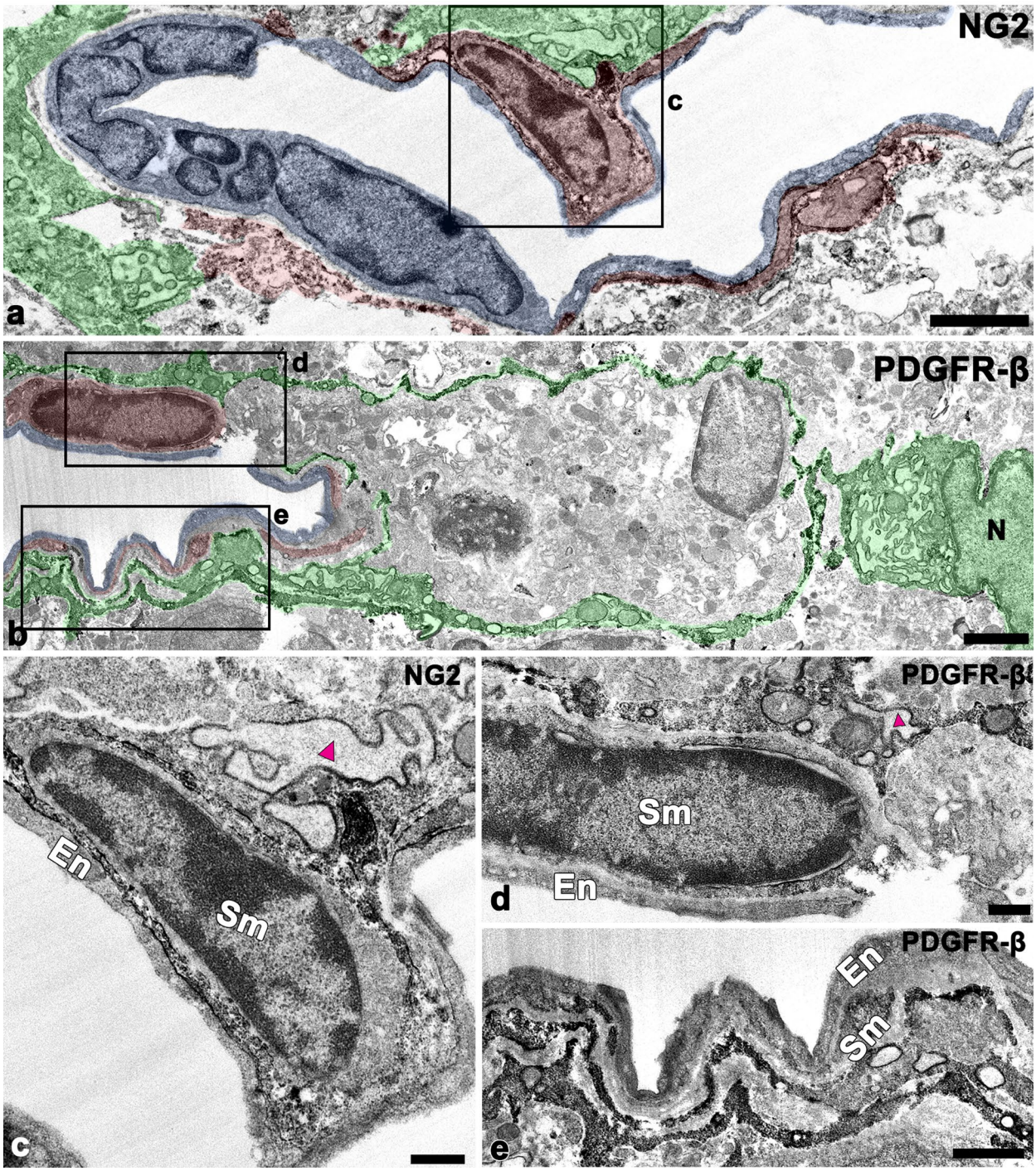

Fig. 3 Comparison of neuron-glia antigen 2 (NG2)- and platelet-derived growth factor receptor beta (PDGFR-β)-positive cells associated with venules using alternatively performed pre-embedding immunoelectron microscopy. Representative images were obtained from the lesion core of the same experimental animal at 3 days post-lesion. **a**, **c** NG2 immunoreactivity, as indicated by highly electron-dense 3,3′-diaminobenzidine tetrahydrochloride (DAB) grains, is specifically associated with the plasma membrane and its adjacent extracellular matrix of smooth muscle cells (Sm; shaded in red) but not with endothelial cells (En; shaded in blue). The boxed area in **a** is enlarged in **c**. Notably, NG2-negative cells (shaded in green) with dilated cisternae of rough endoplasmic reticulum (magenta arrowhead in **c**) are located on the abluminal side of NG2-positive smooth muscle cells. **b**, **d**, **e** PDGFR-β-positive cells (shaded in green) extend long cytoplasmic processes along the outer parts of a smooth muscle cell (Sm; shaded in red) and endothelial cells (En; shaded in blue). Notably, PDGFR-β-positive cells have large euchromatic nuclei (N) and well-developed rough endoplasmic reticulum with dilated cisternae (magenta arrowhead in **d**). The boxed areas in **b** are enlarged in **d** and **e**, respectively. Note that PDGFR-β-positive processes directly abut the abluminal surface of smooth muscle cells and often form a multilayered sheath that covers the smooth muscle cells. Scale bars = 2 μm for **a**, **b**; 1 μm for **e**; 0.5 μm for **c**, **d**

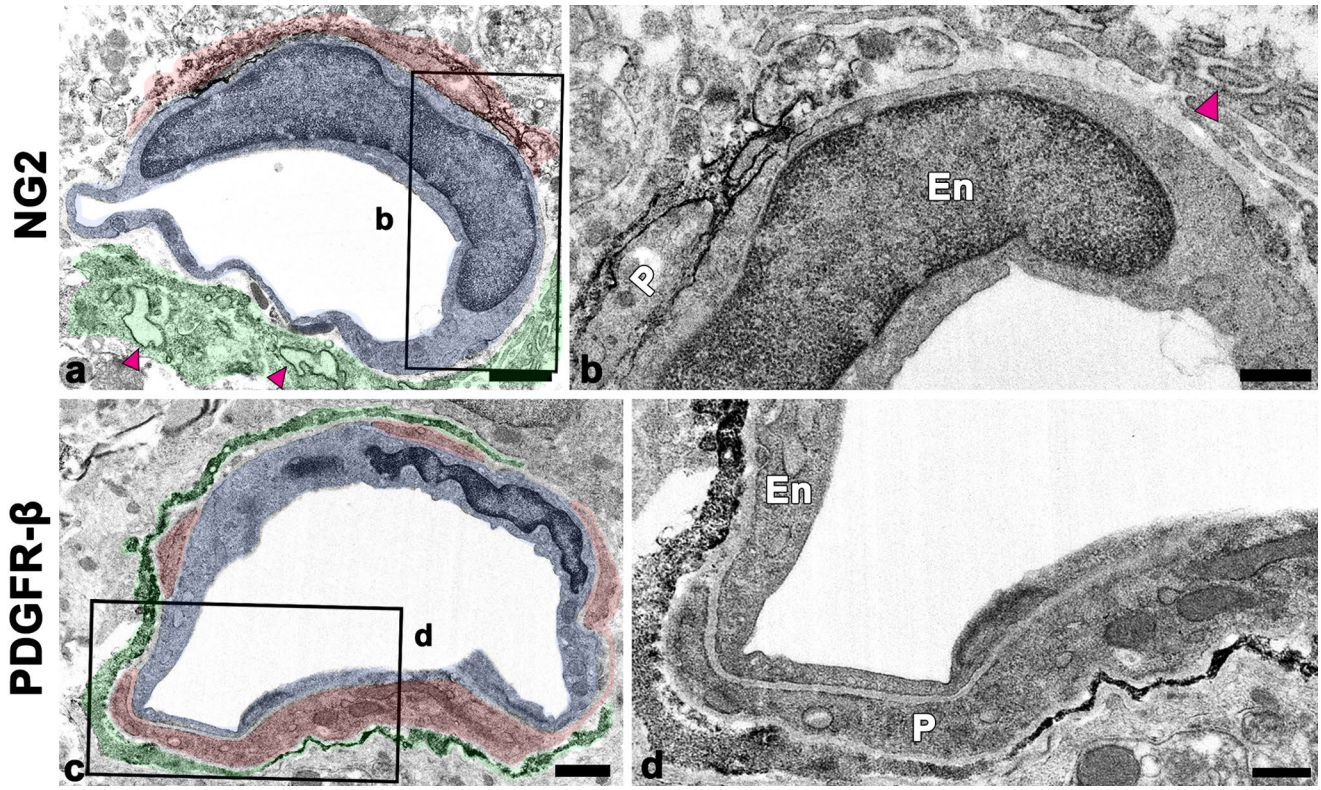

Fig. 4 Comparison of neuron-glia antigen 2 (NG2)- and platelet-derived growth factor receptor beta (PDGFR-β)-positive cells associated with capillaries using alternatively performed pre-embedding immunoelectron microscopy. All images were obtained from the lesion core of the same experimental animal at 3 days post-lesion. **a**, **b** NG2 is specifically localized along the plasma membrane of pericytes (P; shaded in red) of capillaries, which are closely apposed to endothelial cells (En; shaded in blue). The boxed area in **a** is enlarged in **b**. Note that endothelial cells are devoid of NG2. Moreover, note that NG2-negative cells (shaded in green) with dilated cisternae of rough endoplasmic reticulum (magenta arrowheads in **a** and **b**) are located on the abluminal side of NG2-positive pericytes. **c**, **d** PDGFR-β-positive processes directly abut the abluminal surface of pericytes (P; shaded in red) and endothelial cells (En; shaded in blue), both of which are devoid of PDGFR-β. The boxed area in **c** is enlarged in **d**. Data are representative of 20 capillaries from three rats. Scale bars = 1 μm for **a**, **c**; 0.5 μm for **b**, **d**

NG2, PDGFR-β, and Iba1. On 3 days post-lesion, $NG2^+$/$Iba1^-$ cells, namely, NG2 glia, expressed PDGFR-β, while $NG2^+$/$Iba1^+$ activated microglia/macrophages were devoid of PDGFR-β expression (Fig. 6a–d). Seven days post-lesion, the labeling patterns for NG2, PDGFR-β, and Iba1 in the lesion core were similar to those observed on day 3, although there was prominent enrichment of NG2-positive activated microglia/macrophages (Fig. 6e–h). This observation was confirmed by quantitative temporal analysis showing that the numbers of NG2 glia and NG2-positive microglia significantly increased over a 7-day period after lesion induction (Fig. 6i, j). In particular, the number of NG2-positive microglia at 7 days considerably increased when compared with that at the 3-day time point (Fig. 6j). These data indicate that parenchymal NG2-positive cells could be divided into PDGFR-β-positive NG2 glia and PDGFR-β-negative activated microglia/macrophages.

We then determined the ultrastructural morphology of these parenchymal cells using CLEM. Semi-thin sections triple-labeled for NG2, PDGFR-β, and Iba1 were first observed using confocal microscopy, which clearly revealed two types of parenchymal cells, i.e., $NG2^+$/$PDGFR\text{-}\beta^+$ NG2 glia and $NG2^+$/$PDGFR\text{-}\beta^-$ activated microglia/macrophages (Fig. 6k–n). Overlay of the confocal microscopy and transmission electron microscopy data confirmed that activated microglia had triangular nuclei with clumped heterochromatin, whereas NG2 glia had large euchromatic nuclei with prominent nucleoli and well-developed rough endoplasmic reticulum (Fig. 6o–r).

Distributions of and relationship between NG2 and PDGFR-β in the striatum in the late phase following 3-NP injection

Fourteen days after lesion induction, NG2 and PDGFR-β exhibited largely complementary patterns in the lesion core; PDGFR-β expression was associated with vascular profiles and the surrounding web-like structures in the

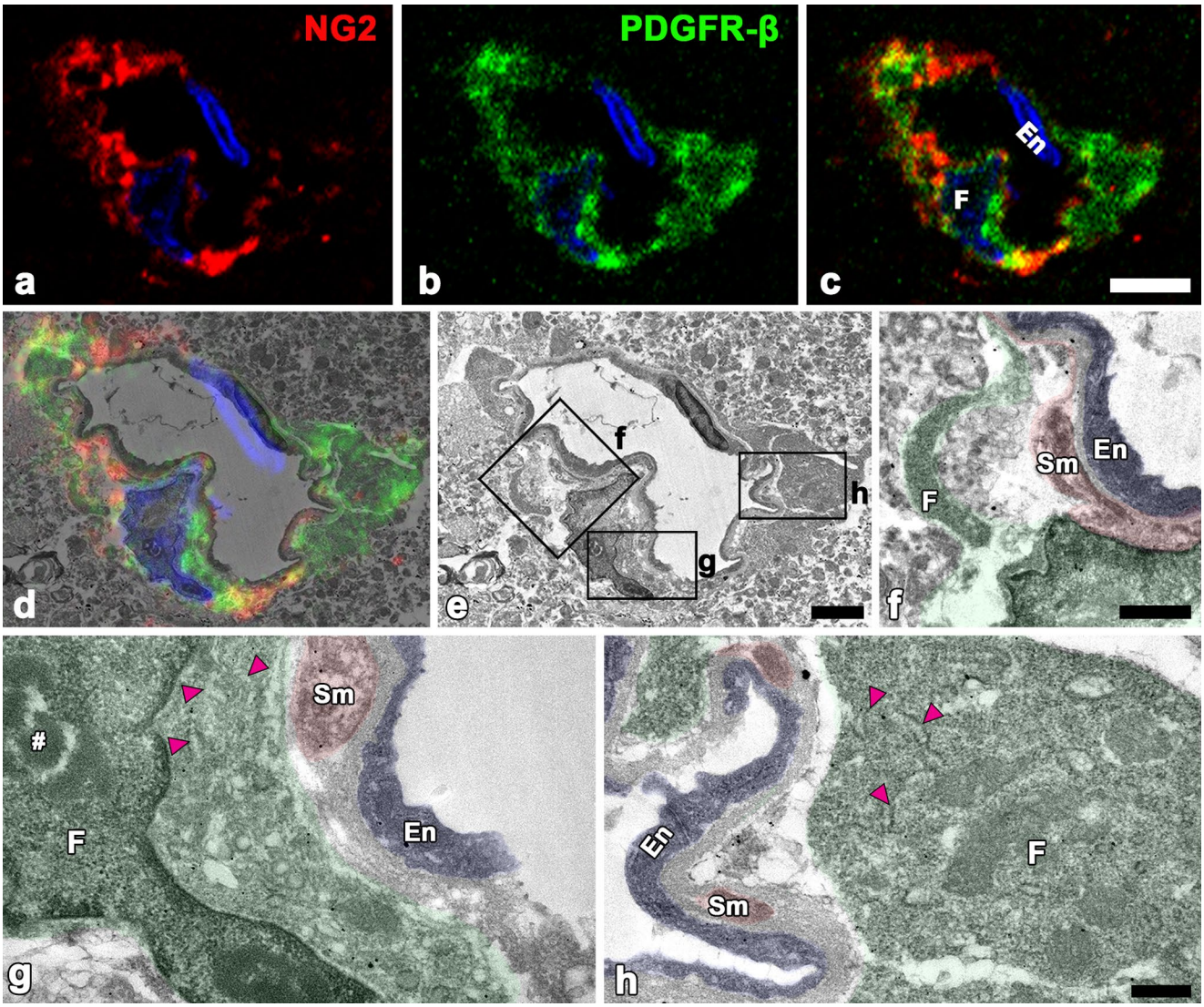

Fig. 5 Phenotypic identification of vessel-associated neuron-glia antigen 2 (NG2)- and platelet-derived growth factor receptor beta (PDGFR-β)-positive cells in the lesion core at 3 days post-lesion using correlative light and electron microscopy. Confocal microscope images of a semi-thin section double-labeled for NG2 and PDGFR-β **a**–**c**, the overlay image of the confocal microscope data **d**, and the corresponding electron microscope image **e**. The boxed areas in **e** are enlarged in **f**–**h**, respectively. Note that NG2 expression is localized in smooth muscle cells (Sm; shaded in red), while PDGFR-β-positive cells (F; shaded in green) are located on the abluminal side of smooth muscle cells and endothelial cells (En; shaded in blue). Note that a PDGFR-β-positive cell has a large euchromatic nucleus with a prominent nucleolus (# in **g**) and well-developed rough endoplasmic reticulum (magenta arrows in **g** and **h**). CLEM image representative from three rats. Cell nuclei appear blue after 4′,6-diamidino-2′-phenylindole (DAPI) staining. Scale bars = 5 µm for **a**–**c**; 2 µm for **d**, **e**; 1 µm for **f**; 0.4 µm for **g**, **h**

extravascular area, while NG2-positive cells were preferentially accumulated in the area between the PDGFR-β-positive structures (Fig. 7a). These complementary patterns of NG2 and PDGFR-β in the lesion core were further supported by the fluorescence intensity profiles of the two signals (Fig. 7b). Triple-labeling with NG2, PDGFR-β, and collagen IV revealed that PDGFR-β and collagen IV generally overlapped in the lesion core, while most NG2-positive cells were located between PDGFR-β-positive extravascular structures (Fig. 7c–f). Collagen IV and collagen I, the principal type of collagen, had nearly coinciding distributions in the lesion core (Fig. 7g, h). Triple-labeling with NG2, PDGFR-β, and Iba1 showed that these NG2-positive cells were indeed activated microglia/macrophages, despite $NG2^{+}$/PDGFR-β^{+} NG2 glia still being present (Fig. 7i–l).

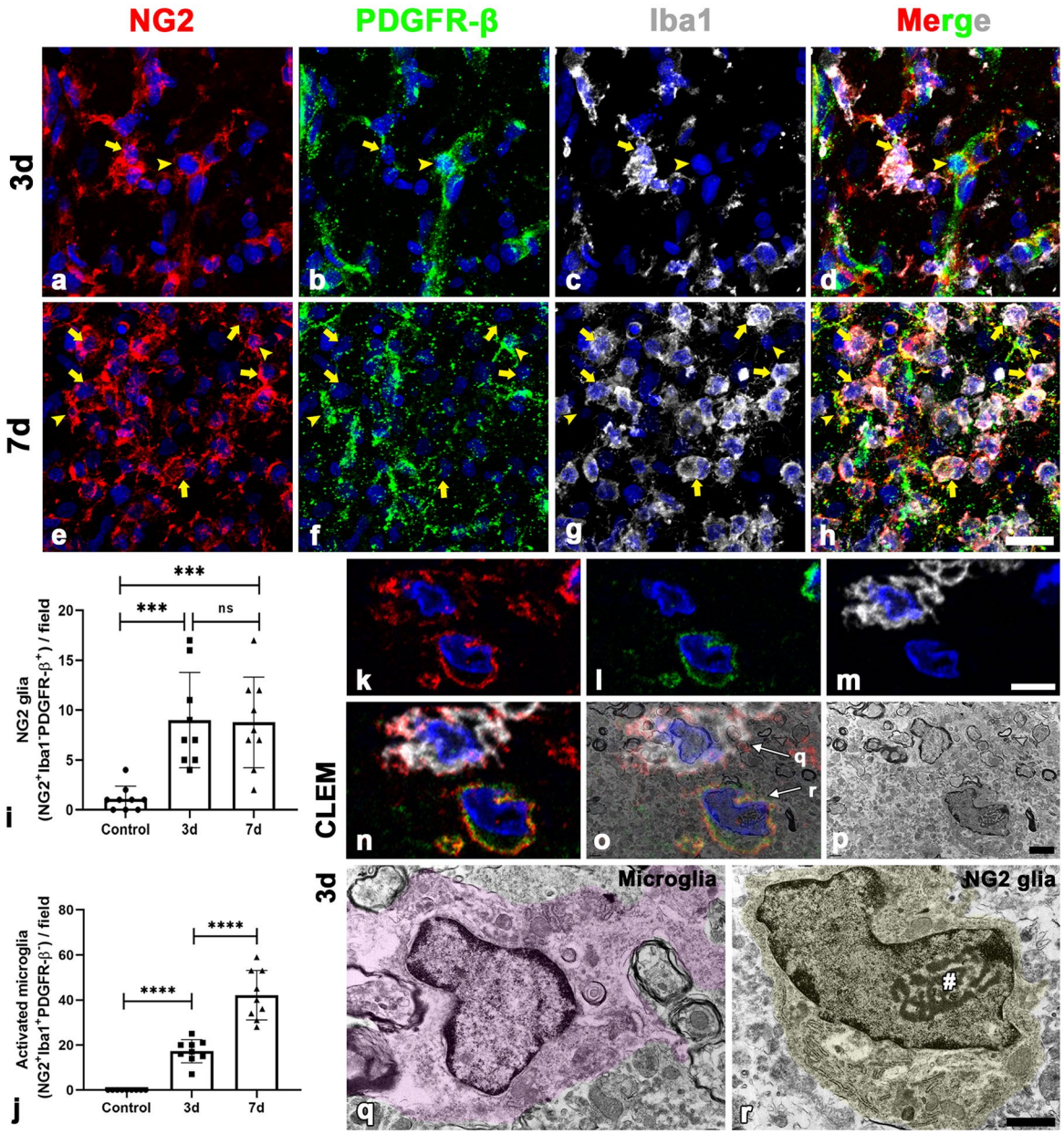

Fig. 6 Phenotypic identification and ultrastructural characterization of parenchymal cells expressing neuron-glia antigen 2 (NG2) and platelet-derived growth factor receptor beta (PDGFR-β) in the lesion core on days 3 and 7 after 3-nitropropionic acid (3-NP) injection. **a**–**d** Triple-labeling for PDGFR-β, NG2, and ionized calcium-binding adaptor molecule 1 (Iba1) 3 days post-lesion shows that NG2/PDGFR-β double-labeled cells (arrowheads) in the extravascular area, most likely NG2 glia, are not labeled with Iba1. Note that NG2-positive activated microglia/macrophages (arrows) are devoid of PDGFR-β. **e**–**h** Triple-labeling for PDGFR-β, NG2, and Iba1 7 days post-lesion shows that two types of parenchymal cells, i.e., $NG2^+$/$PDGFR\text{-}\beta^+$ NG2 glia (arrowheads) and $NG2^+$/$PDGFR\text{-}\beta^-$ activated microglia/macrophages (arrows), are clearly distinguishable. Furthermore, note the more prominent enrichment of NG2-positive activated microglia/macrophages at 7 days post-lesion, in comparison to day 3 post-lesion. **i, j** Quantitative temporal analysis showing a significant increase in the numbers of NG2 glia ($NG2^+$/$Iba1^-$/$PDGFR\text{-}\beta^+$ cells) and NG2-positive microglia ($NG2^+$/$Iba1^+$/$PDGFR\text{-}\beta^-$ cells) over a 7-day period after lesion induction. $n = 3$ rats per group. Data are expressed as mean ± SEM. ns, not significant; $^{***}P < 0.001$, $^{****}P < 0.0001$; one-way ANOVA followed by Tukey's multiple comparison test. **k**–**r** Representative correlative light- and electron-microscopic images show the ultrastructural characterization of parenchymal cells expressing NG2 and PDGFR-β. Confocal microscopic images of a semi-thin section triple-labeled for NG2, PDGFR-β, and Iba1 **k**–**n**, the overlay image of the confocal microscope data **o**, and the corresponding electron microscope image **p**. **q**, **r** Higher magnification views of $NG2^+$/$PDGFR\text{-}\beta^-$ microglia and $NG2^+$/$PDGFR\text{-}\beta^+$ NG2 glia, respectively. Note that the former has a triangular nucleus with highly clumped heterochromatin, whereas the latter has a large euchromatic nucleus with a prominent nucleolus (# in **r**) and cytoplasm containing well-developed rough endoplasmic reticulum. Light microscopy and CLEM data from three rats per group are presented. Cell nuclei appear blue after 4′,6-diamidino-2′-phenylindole (DAPI) staining. Scale bars = 20 µm for **a**–**h**; 5 µm for **k**–**m**; 2 µm for **n**–**p**; 1 µm for **q**–**r**

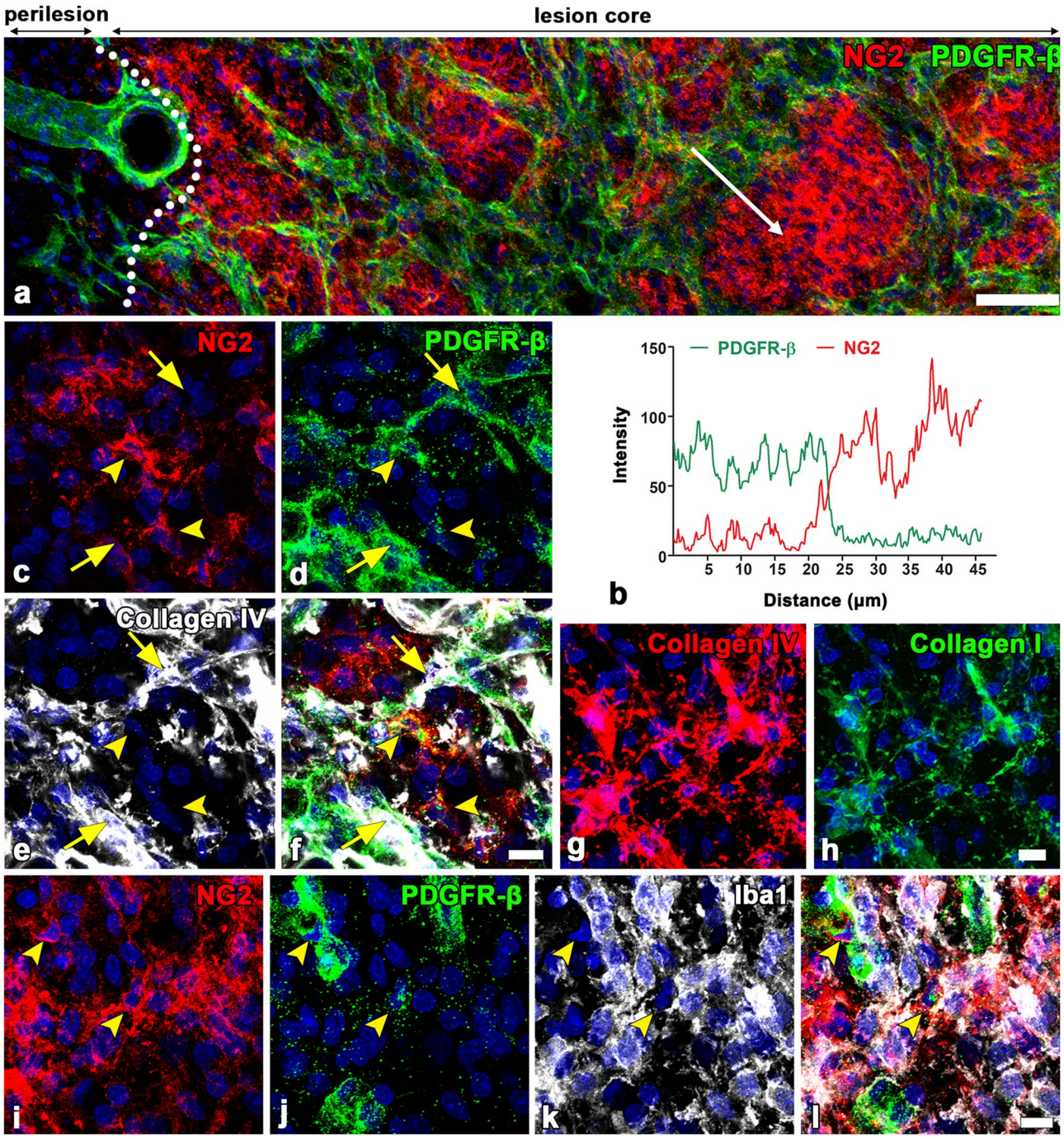

Fig. 7 Spatial distribution of and relationship between neuron-glia antigen 2 (NG2) and platelet-derived growth factor receptor beta (PDGFR-β) in the lesioned striatum on day 14 after 3-nitropropionic acid (3-NP) injection. **a** Double-labeling for NG2 and PDGFR-β shows that PDGFR-β expression is associated with vascular profiles and the surrounding web-like extravascular structures, while NG2-positive cells are preferentially observed between the PDGFR-β-positive structures. The dotted line indicates the border between the lesion core and the perilesional area (perilesion). **b** Fluorescence intensity profiles of NG2- and PDGFR-β-positive signals along the indicated area (arrow in **a**) show that both signals have largely complementary patterns. **c–f** Triple-labeling with NG2, PDGFR-β, and collagen IV in the lesion core shows that PDGFR-β is closely associated with collagen IV within extravascular networks (arrows), while most NG2-positive cells are located among PDGFR-β-positive structures. Note that $NG2^+$/$PDGFR\text{-}\beta^+$ NG2 glia (arrowheads) are still observed. **g–h** Double-labeling with collagen IV and collagen I shows that the expression of the two collagen proteins generally overlap in the lesion core. **i–l** Triple-labeling for NG2, PDGFR-β, and ionized calcium-binding adaptor molecule 1 (Iba1) in the lesion core shows that most NG2-positive cells in the extravascular area are indeed activated microglia/macrophages despite the presence of some $NG2^+$/$PDGFR\text{-}\beta^+$ NG2 glia (arrowheads). Light microscopy data are representative from three rats. Cell nuclei appear blue after 4′,6-diamidino-2′-phenylindole (DAPI) staining. Scale bars = 50 μm for **a**; 10 μm for **c–l**

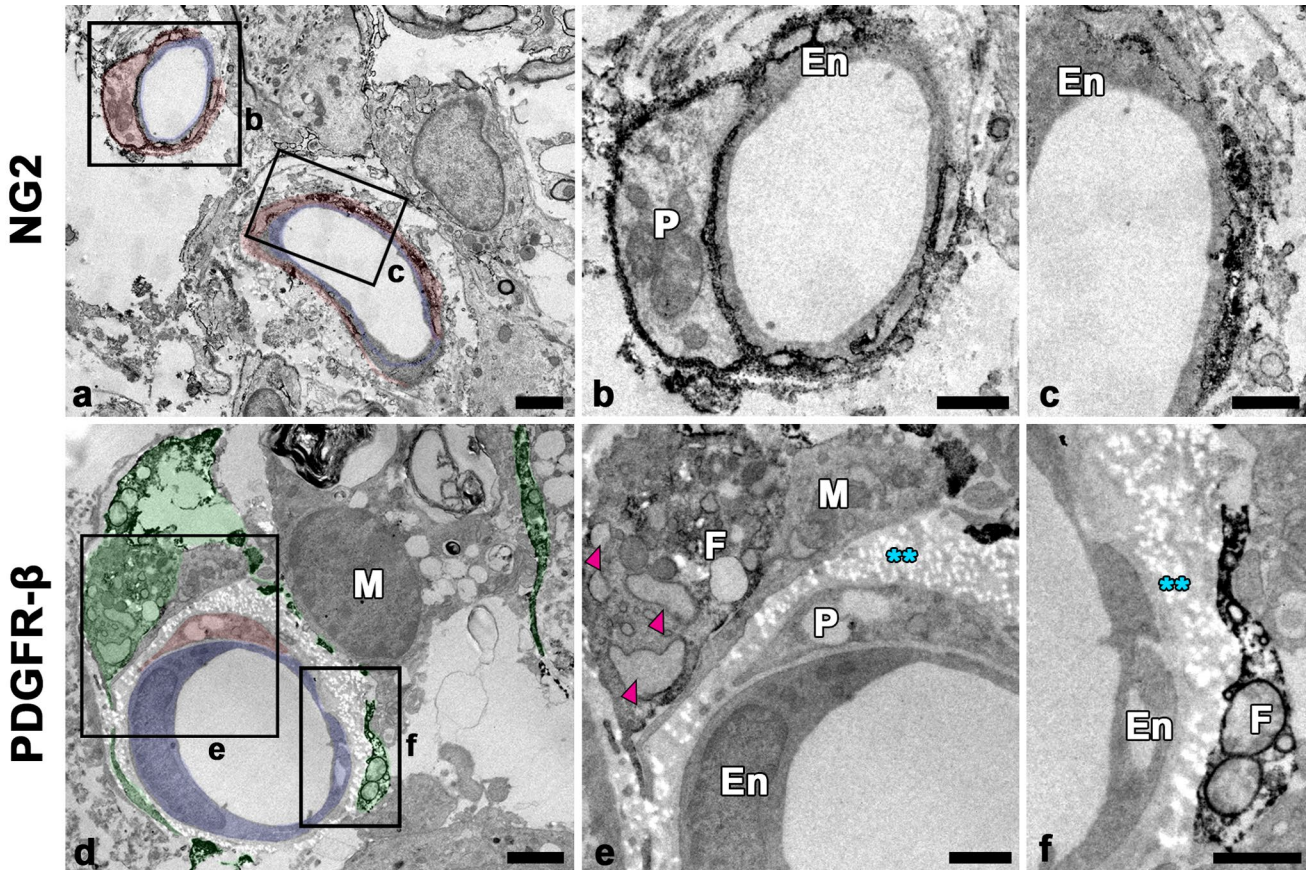

Fig. 8 Ultrastructural analysis of vessel-associated neuron-glia antigen 2 (NG2)- and platelet-derived growth factor receptor beta (PDGFR-β)-positive cells in the lesion core 14 days post-lesion using alternatively performed pre-embedding immunoelectron microscopy. **a**–**c** Electron-dense NG2 staining is specifically associated with the plasma membranes of pericytes (P; shaded in red) but not with endothelial cells (En; shaded in blue) of capillaries. The boxed areas in **a** are enlarged in **b** and **c**, respectively. **d**–**f** PDGFR-β-positive cytoplasmic processes (F; shaded in green) directly abut the abluminal surface of pericytes (P; shaded in red) and endothelial cells (En; shaded in blue) of capillaries but are also located at a distance from the vasculature. PDGFR-β-positive processes have morphological features typical of perivascular fibroblasts, such as well-developed rough endoplasmic reticulum with dilated cisterns (magenta arrowheads in **e**), and a close association with collagen fibrils (double asterisks in **e** and **f**). Note that PDGFR-β-positive processes are in close apposition to brain macrophages (M). The boxed areas in **d** are enlarged in **e** and **f**, respectively. Data are representative of 30 capillaries from three rats. Scale bars = 2 µm for **a**, **d**; 1 µm for **b**, **c**, **e**, **f**

To characterize how vessel-associated cells expressing the two proteins changed over time, we investigated the ultrastructural morphology and spatial relationships of these cells in the lesion core 14 days post-lesion. Alternatively performed pre-embedding immunoelectron microscopy demonstrated that electron-dense NG2 staining was still localized along the plasma membranes of capillary pericytes (Fig. 8a–c), while slender PDGFR-β-positive cytoplasmic processes directly abutted the abluminal surface of pericytes but were also located at a distance from the vasculature with close apposition with brain macrophages (Fig. 8d–f). They still showed morphological characteristics typical of perivascular fibroblast, such as well-developed rough endoplasmic reticulum with dilated cisterns, and a close association with collagen fibrils (Fig. 8d–f). In each of the 30 capillaries analyzed, all of the pericytes expressed NG2 but not PDGFR-β.

Discussion

NG2 and PDGFR-β are widely used as markers for pericytes, yet the validity of this approach remains controversial due to the delicate nature of perivascular structures (Armulik et al. 2011; Krueger and Bechmann 2010; Lindahl et al. 1997; Riew et al. 2020; Schultz et al. 2017; Smyth et al. 2018; Winkler et al. 2010). In the present study, we elucidated the identities and distributions of vessel-associated cells expressing NG2 and PDGFR-β and found, surprisingly, that these molecules labeled different vascular mural cells; NG2 labeled pericytes and smooth muscle cells, whereas PDGFR-β did label neither pericytes nor smooth muscle cells but instead clearly labeled perivascular adventitial fibroblast-like cells. Furthermore, we established the identity of heterogeneous populations of NG2- and

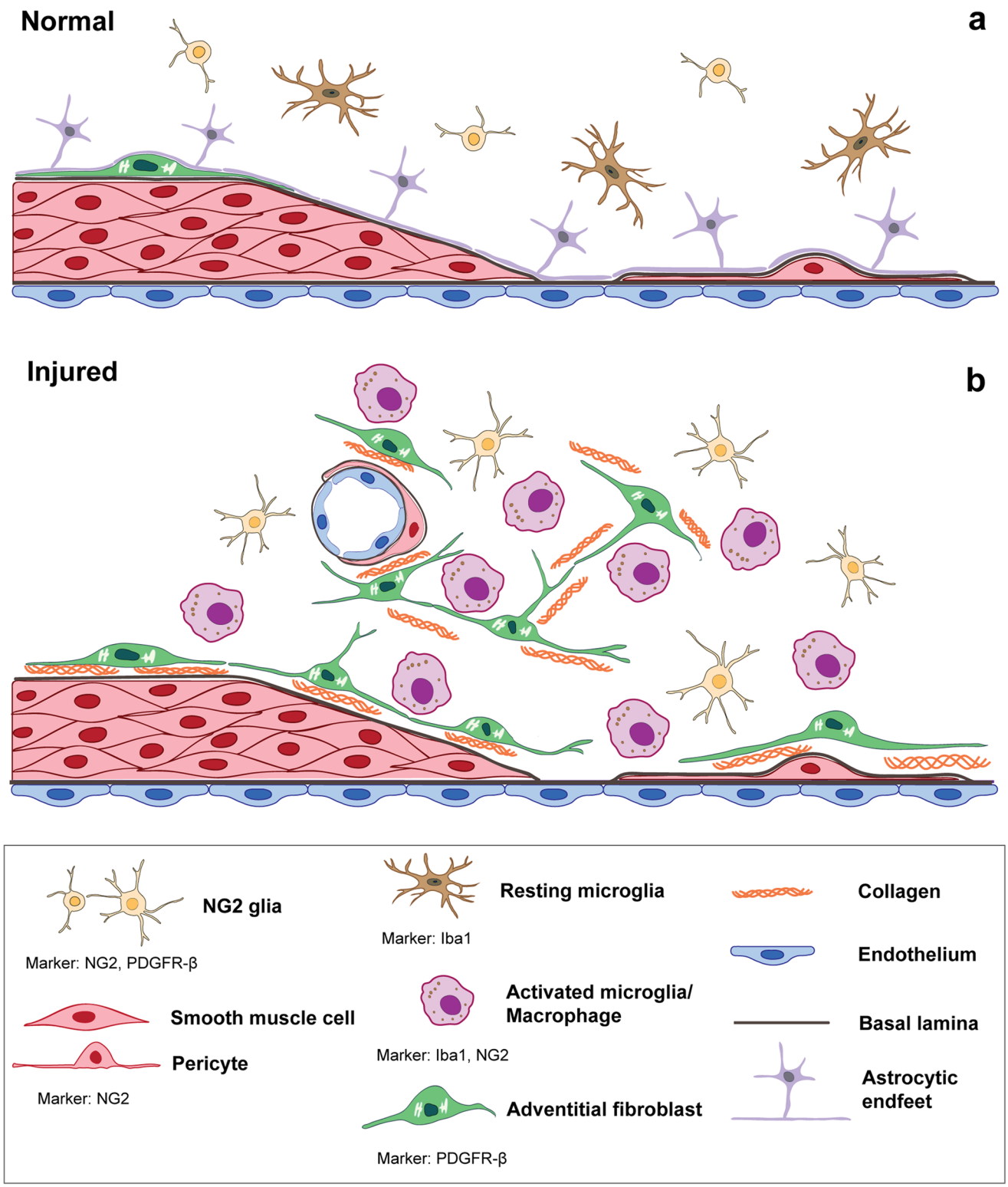

PDGFR-β-positive parenchymal cells at regional, cellular, and subcellular levels in the control and lesioned striatum.

In addition to vascular mural cells, both NG2 and PDGFR-β are expressed by diverse cell types in the healthy and diseased CNS. NG2 is induced in activated microglia/macrophages after CNS insults, as well as its obvious expression by NG2 glia in the adult brain (Dimou and Gallo 2015; Jin et al. 2018, 2020; Nishiyama et al. 1997; Ozerdem et al. 2001). PDGFR-β is expressed by perivascular stromal cells, perivascular fibroblasts, and even NG2

Fig. 9 Schematic representation of the dynamic distribution of neuron-glia antigen 2 (NG2) and platelet-derived growth factor receptor beta (PDGFR-β) in the lesion core of the striatum following 3-nitropropionic acid (3-NP) treatment. **a** In the saline-treated control striatum, vessel-associated cells expressing NG2 are pericytes and smooth muscle cells, which are surrounded by the basal lamina, whereas PDGFR-β-positive cells are adventitial fibroblasts that are localized on the abluminal side of the smooth muscle cells of larger caliber vessels. Parenchymal cells expressing both proteins are resting NG2 glia. Note that PDGFR-β-positive adventitial fibroblasts are surrounded by the glia limitans of astroglial processes. **b** At 14 days post-lesion, when a degenerating glia limitans is evident in the lesion core, pericytes and smooth muscle cells expressing NG2 still reside within the perivascular space, whereas PDGFR-β-positive fibroblasts in the vascular adventitia migrate into the injured parenchyma and form an extravascular network, despite the ongoing association with the vasculature. Cells expressing PDGFR-β are closely associated with collagen fibrils. Reactive NG2 glia still express both NG2 and PDGFR-β, while NG2 is also induced in activated microglia/macrophages. Iba1, ionized calcium-binding adaptor molecule 1

glia in the injured CNS (Fernandez-Klett et al. 2013; Riew et al. 2018; Soderblom et al. 2013). We demonstrated that NG2 and PDGFR-β had overlapping yet clearly distinguishable expression patterns within the striatal parenchyma after brain insults. The CLEM analysis identified two types of parenchymal cells; $NG2^+$/PDGFR-β^+ cells, namely, NG2 glia, and $NG2^+$/PDGFR-β^- activated microglia/macrophages are clearly distinguishable. The former exhibited the characteristic ultrastructure of reactive NG2 glia, i.e., large euchromatic nuclei with prominent nucleoli and well-developed rough endoplasmic reticulum (see Fig. 6p), as reported previously (Jin et al. 2018, 2020; Nishiyama et al. 1997). On the other hand, the latter had morphological features typical of activated microglia, consistent with our previous observations (Jin et al. 2018, 2020; Riew et al. 2018). Thus, based on the parenchymal distribution patterns of these two molecules, the complementary use of PDGFR-β could be beneficial to mark solely NG2 glia in the lesioned striatum. Figure 9 summarizes our light- and electron-microscopic analysis of vascular and parenchymal distributions of NG2 and PDGFR-β in both the control and lesioned striatum.

Most noteworthy, we found that NG2 and PDGFR-β were neither exclusive nor specific markers for pericytes. Previous research has identified the co-expression of both molecules in vascular mural cells using transcriptomic analysis and light microscopy. However, our study is hitherto the first to directly compare and clarify the natural expression pattern of these two molecules at both the light- and electron-microscopic levels without using genetically modified animals (Armulik et al. 2011; He et al. 2016; Lindahl et al. 1997; Sweeney et al. 2016; Vanlandewijck et al. 2018; Winkler et al. 2010). Although NG2 and PDGFR-β revealed spatial differences even at the light-microscopic level (Fig. 2q–t), their exact cellular identities within vascular walls were difficult to establish due to the narrow nature of the perivascular space, the thin pericytic processes (2 μm thick or less), and the closely attached vascular mural cells (Attwell et al. 2016; Krueger and Bechmann 2010). Nevertheless, our immunoelectron microscopy and CLEM images clearly distinguished between NG2-labeled smooth muscle cells and pericytes, whereas PDGFR-β-positive perivascular fibroblasts were located abluminal to NG2-positive cells. NG2 immunoreactivity was conspicuously observed along the cell membranes of smooth muscle cells and pericytes, which is attributable to the inaccurate discrimination from PDGFR-β+ perivascular fibroblasts in light-microscopic images. Thus, particular care should be taken in applying them as markers for these vascular mural cells using light microscopy.

Interestingly, the vascular expression of NG2 and PDGFR-β in the injured striatum exhibited characteristic spatiotemporal patterns during the post-injury period. PDGFR-β–positive perivascular fibroblasts were confined to large-caliber vessels in the healthy brain, but they expanded to almost all vessels after the injury at 3–7 days post-lesion. Although extravascular PDGFR-β expression increased at 7 days post-lesion, mesh-like networks and close correlation with extravascular collagen fibers were more evident at 14 days post-lesion. These networks of processes and collagen deposition correspond to the fibrotic scar formation, consistent with our previous finding (Riew et al. 2018). Thus, our data suggest that PDGFR-β-positive perivascular fibroblasts may start to migrate from the vascular adventitia into the injured parenchyma at days 3–7 post-lesion and form a fibrotic scar by 14 days.

On the other hand, NG2 expression in vascular smooth muscle cells and pericytes prominently increased after the injury, but their localization was restricted to the vasculature at 14 days post-lesion. Birbrair et al. reported that after traumatic brain injury, NG2DsRed+ pericytes and PDGFR-β+ cells both accumulate around the fibrotic scar area but do not show overlapping patterns, suggesting distinct populations of each cell type (Birbrair et al. 2014). In addition, status epilepticus induces alterations in the coverage of NG2DsRed+ cells around cerebral vasculature, while these cells are in close contact with fibrotic scar-forming PDGFR-β+ cells, and vascular pericytes detached from tumor microvasculature acquire fibroblasts phenotypes upon stimulation by specific signaling ligands, like PDGF-BB (Hosaka et al. 2016; Klement et al. 2019; Milesi et al. 2014). It is conceivable that upon injury, a subpopulation of NG2+ pericytes might contribute to the pool of PDGFR-β+ perivascular fibroblasts. It is also plausible that the upregulation of NG2 in vascular mural cells indicates that their role in vascular remodeling or morphogenesis in the lesion core differs from that of PDGFR-β+ perivascular fibroblasts (Fukushi et al. 2004; Gibby et al. 2012; Ozerdem et al. 2001; Stallcup et al. 2016; Yadavilli et al. 2016). Furthermore, $NG2^+$ parenchymal cells, i.e., NG2 glia and activated microglia/macrophages,

proliferated and accumulated among the PDGFR-β-positive fibrous networks. Mounting evidence suggests that these cells could intervene actively in tissue remodeling and regeneration via secretion of cytokines like transforming growth factor-beta and galectin-3 (Braga et al. 2015; Jin et al. 2018; Riew et al. 2018; Vernon et al. 2010; Zhu et al. 2015, 2016). It is likely that NG2 glia, activated microglia/macrophages, and PDGFR-β-positive perivascular fibroblasts interact to form the fibrotic scar in the lesion core after CNS insults.

In conclusion, our data clearly provided evidence for distinct localizations of vascular mural cells expressing NG2 and PDGFR-β. NG2 was consistently expressed in pericytes and smooth muscle cells during the post-injury time, whereas PDGFR-β labeled adventitial fibroblasts were located at a distance from the vasculature at later time points post-lesion. In addition, NG2 and PDGFR-β were expressed in parenchymal cells in the control and lesioned striatum. Both markers were expressed in resting and reactive NG2 glia, but only NG2 was induced in activated microglia/macrophages. These data provide detailed and precise information regarding the appropriate markers for vascular mural cells in the healthy and injured brain, suggesting that the cells directly responsible for fibrotic scar formation are most likely PDGFR-β-positive adventitial fibroblasts rather than NG2-positive pericytes.

Supplementary Information The online version contains supplementary material available at https://doi.org/10.1007/s00441-021-03438-3.

Funding This research was supported by the grant from the National Research Foundation of Korea (NRF) (grant number NRF- 2020R1A2B5B01001442).

Declarations

Ethics Approval All interventions and animal care provisions were in accordance with the Laboratory Animals Welfare Act, the Guide for the Care and Use of Laboratory Animals, and the Guidelines and Policies for Rodent Survival Surgery provided by the IACUC (Institutional Animal Care and Use Committee) at the College of Medicine, The Catholic University of Korea (approval number CUMS-2020-0041-01).

Conflict of interest The authors declare that they have no competing interest.

References

Armulik A, Genove G, Betsholtz C (2011) Pericytes: developmental, physiological, and pathological perspectives, problems, and promises. Dev Cell 21:193–215

Armulik A, Genove G, Mae M, Nisancioglu MH, Wallgard E, Niaudet C, He L, Norlin J, Lindblom P, Strittmatter K, Johansson BR, Betsholtz C (2010) Pericytes regulate the blood-brain barrier. Nature 468:557–561

Attwell D, Mishra A, Hall CN, O'Farrell FM, Dalkara T (2016) What is a pericyte? J Cereb Blood Flow Metab 36:451–455

Birbrair A, Zhang T, Files DC, Mannava S, Smith T, Wang ZM, Messi ML, Mintz A, Delbono O (2014) Type-1 pericytes accumulate after tissue injury and produce collagen in an organ-dependent manner. Stem Cell Res Ther 5:122

Braga TT, Agudelo JS, Camara NO (2015) Macrophages during the fibrotic process: M2 as friend and foe. Front Immunol 6:602

Bu J, Akhtar N, Nishiyama A (2001) Transient expression of the NG2 proteoglycan by a subpopulation of activated macrophages in an excitotoxic hippocampal lesion. Glia 34:296–310

Casella GT, Bunge MB, Wood PM (2004) Improved immunocytochemical identification of neural, endothelial, and inflammatory cell types in paraffin-embedded injured adult rat spinal cord. J Neurosci Methods 139:1–11

Cha JH, Wee HJ, Seo JH, Ahn BJ, Park JH, Yang JM, Lee SW, Kim EH, Lee OH, Heo JH, Lee HJ, Gelman IH, Arai K, Lo EH, Kim KW (2014) AKAP12 mediates barrier functions of fibrotic scars during CNS repair. PLoS ONE 9:e94695

Choi JH, Riew TR, Kim HL, Jin X, Lee MY (2017) Desmin expression profile in reactive astrocytes in the 3-nitropropionic acid-lesioned striatum of rat: Characterization and comparison with glial fibrillary acidic protein and nestin. Acta Histochem 119:795–803

Dimou L, Gallo V (2015) NG2-glia and their functions in the central nervous system. Glia 63:1429–1451

Duran-Vilaregut J, Del Valle J, Manich G, Junyent F, Camins A, Pallas M, Pelegri C, Vilaplana J (2010) Systemic administration of 3-nitropropionic acid points out a different role for active caspase-3 in neurons and astrocytes. Neurochem Int 56:443–450

Fernandez-Klett F, Potas JR, Hilpert D, Blazej K, Radke J, Huck J, Engel O, Stenzel W, Genove G, Priller J (2013) Early loss of pericytes and perivascular stromal cell-induced scar formation after stroke. J Cereb Blood Flow Metab 33:428–439

Fernandez-Klett F, Priller J (2014) The fibrotic scar in neurological disorders. Brain Pathol 24:404–413

Fukushi J, Makagiansar IT, Stallcup WB (2004) NG2 proteoglycan promotes endothelial cell motility and angiogenesis via engagement of galectin-3 and alpha3beta1 integrin. Mol Biol Cell 15:3580–3590

Garbelli R, de Bock F, Medici V, Rousset MC, Villani F, Boussadia B, Arango-Lievano M, Jeanneteau F, Daneman R, Bartolomei F, Marchi N (2015) PDGFRbeta(+) cells in human and experimental neuro-vascular dysplasia and seizures. Neuroscience 306:18–27

Gibby K, You WK, Kadoya K, Helgadottir H, Young LJ, Ellies LG, Chang Y, Cardiff RD, Stallcup WB (2012) Early vascular deficits are correlated with delayed mammary tumorigenesis in the MMTV-PyMT transgenic mouse following genetic ablation of the NG2 proteoglycan. Breast Cancer Res 14:R67

Goritz C, Dias DO, Tomilin N, Barbacid M, Shupliakov O, Frisen J (2011) A pericyte origin of spinal cord scar tissue. Science 333:238–242

Hamilton BF, Gould DH (1987) Nature and distribution of brain lesions in rats intoxicated with 3-nitropropionic acid: a type of hypoxic (energy deficient) brain damage. Acta Neuropathol 72:286–297

He L, Vanlandewijck M, Raschperger E, Andaloussi Mae M, Jung B, Lebouvier T, Ando K, Hofmann J, Keller A, Betsholtz C (2016) Analysis of the brain mural cell transcriptome. Sci Rep 6:35108

Hesp ZC, Yoseph RY, Suzuki R, Jukkola P, Wilson C, Nishiyama A, McTigue DM (2018) Proliferating NG2-cell-dependent angiogenesis and scar formation alter axon growth and functional recovery after spinal cord injury in mice. J Neurosci 38:1366–1382

Hosaka K, Yang Y, Seki T, Fischer C, Dubey O, Fredlund E, Hartman J, Religa P, Morikawa H, Ishii Y, Sasahara M, Larsson O, Cossu G, Cao R, Lim S, Cao Y (2016) Pericyte-fibroblast transition promotes tumor growth and metastasis. Proc Natl Acad Sci U S A 113:E5618-5627

Jin X, Riew TR, Kim HL, Choi JH, Lee MY (2018) Morphological characterization of NG2 glia and their association with neuroglial cells in the 3-nitropropionic acid-lesioned striatum of rat. Sci Rep 8:5942

Jin X, Riew TR, Kim S, Kim HL, Lee MY (2020) Spatiotemporal profile and morphological changes of NG2 glia in the CA1 region of the rat hippocampus after transient forebrain ischemia. Exp Neurobiol 29:50–69

Jones LL, Sajed D, Tuszynski MH (2003) Axonal regeneration through regions of chondroitin sulfate proteoglycan deposition after spinal cord injury: a balance of permissiveness and inhibition. J Neurosci 23:9276–9288

Klement W, Blaquiere M, Zub E, deBock F, Boux F, Barbier E, Audinat E, Lerner-Natoli M, Marchi N (2019) A pericyte-glia scarring develops at the leaky capillaries in the hippocampus during seizure activity. Epilepsia 60:1399–1411

Krueger M, Bechmann I (2010) CNS pericytes: concepts, misconceptions, and a way out. Glia 58:1–10

Kyyriainen J, Ekolle Ndode-Ekane X, Pitkanen A (2017) Dynamics of PDGFRbeta expression in different cell types after brain injury. Glia 65:322–341

Lindahl P, Johansson BR, Leveen P, Betsholtz C (1997) Pericyte loss and microaneurysm formation in PDGF-B-deficient mice. Science 277:242–245

Matsumoto H, Kumon Y, Watanabe H, Ohnishi T, Shudou M, Chuai M, Imai Y, Takahashi H, Tanaka J (2008) Accumulation of macrophage-like cells expressing NG2 proteoglycan and Iba1 in ischemic core of rat brain after transient middle cerebral artery occlusion. J Cereb Blood Flow Metab 28:149–163

Milesi S, Boussadia B, Plaud C, Catteau M, Rousset MC, De Bock F, Schaeffer M, Lerner-Natoli M, Rigau V, Marchi N (2014) Redistribution of PDGFRbeta cells and NG2DsRed pericytes at the cerebrovasculature after status epilepticus. Neurobiol Dis 71:151–158

Mu S, Liu B, Ouyang L, Zhan M, Chen S, Wu J, Chen J, Wei X, Wang W, Zhang J, Lei W (2016) Characteristic changes of astrocyte and microglia in rat striatum induced by 3-NP and MCAO. Neurochem Res 41:707–714

Nishiyama A, Yu M, Drazba JA, Tuohy VK (1997) Normal and reactive NG2+ glial cells are distinct from resting and activated microglia. J Neurosci Res 48:299–312

Ozerdem U, Grako KA, Dahlin-Huppe K, Monosov E, Stallcup WB (2001) NG2 proteoglycan is expressed exclusively by mural cells during vascular morphogenesis. Dev Dyn 222:218–227

Riew TR, Choi JH, Kim HL, Jin X, Lee MY (2018) PDGFR-beta-positive perivascular adventitial cells expressing nestin contribute to fibrotic scar formation in the striatum of 3-NP intoxicated rats. Front Mol Neurosci 11:402

Riew TR, Jin X, Kim HL, Kim S, Lee MY (2020) Ultrastructural and molecular characterization of platelet-derived growth factor beta-positive leptomeningeal cells in the adult rat brain. Mol Neurobiol 57:1484–1501

Riew TR, Kim HL, Jin X, Choi JH, Shin YJ, Kim JS, Lee MY (2017) Spatiotemporal expression of osteopontin in the striatum of rats subjected to the mitochondrial toxin 3-nitropropionic acid correlates with microcalcification. Sci Rep 7:45173

Schultz N, Byman E, Fex M, Wennström M (2017) Amylin alters human brain pericyte viability and NG2 expression. J Cereb Blood Flow Metab 37:1470–1482

Smyth LCD, Rustenhoven J, Scotter EL, Schweder P, Faull RLM, Park TIH, Dragunow M (2018) Markers for human brain pericytes and smooth muscle cells. J Chem Neuroanat 92:48–60

Soderblom C, Luo X, Blumenthal E, Bray E, Lyapichev K, Ramos J, Krishnan V, Lai-Hsu C, Park KK, Tsoulfas P, Lee JK (2013) Perivascular fibroblasts form the fibrotic scar after contusive spinal cord injury. J Neurosci 33:13882–13887

Stallcup WB, You WK, Kucharova K, Cejudo-Martin P, Yotsumoto F (2016) NG2 Proteoglycan-dependent contributions of pericytes and macrophages to brain tumor vascularization and progression. Microcirculation 23:122–133

Sweeney MD, Ayyadurai S, Zlokovic BV (2016) Pericytes of the neurovascular unit: key functions and signaling pathways. Nat Neurosci 19:771–783

Vanlandewijck M, He L, Mae MA, Andrae J, Ando K, Del Gaudio F, Nahar K, Lebouvier T, Lavina B, Gouveia L, Sun Y, Raschperger E, Rasanen M, Zarb Y, Mochizuki N, Keller A, Lendahl U, Betsholtz C (2018) A molecular atlas of cell types and zonation in the brain vasculature. Nature 554:475–480

Vernon MA, Mylonas KJ, Hughes J (2010) Macrophages and renal fibrosis. Semin Nephrol 30:302–317

Winkler EA, Bell RD, Zlokovic BV (2010) Pericyte-specific expression of PDGF beta receptor in mouse models with normal and deficient PDGF beta receptor signaling. Mol Neurodegener 5:32

Wullner U, Young AB, Penney JB, Beal MF (1994) 3-Nitropropionic acid toxicity in the striatum. J Neurochem 63:1772–1781

Yadavilli S, Hwang EI, Packer RJ, Nazarian J (2016) The role of NG2 proteoglycan in glioma. Transl Oncol 9:57–63

Yoshioka N, Hisanaga S, Kawano H (2010) Suppression of fibrotic scar formation promotes axonal regeneration without disturbing blood-brain barrier repair and withdrawal of leukocytes after traumatic brain injury. J Comp Neurol 518:3867–3881

Zhu L, Xiang P, Guo K, Wang A, Lu J, Tay SS, Jiang H, He BP (2012) Microglia/monocytes with NG2 expression have no phagocytic function in the cortex after LPS focal injection into the rat brain. Glia 60:1417–1426

Zhu Y, Soderblom C, Krishnan V, Ashbaugh J, Bethea JR, Lee JK (2015) Hematogenous macrophage depletion reduces the fibrotic scar and increases axonal growth after spinal cord injury. Neurobiol Dis 74:114–125

Zhu Z, Ding J, Ma Z, Iwashina T, Tredget EE (2016) Systemic depletion of macrophages in the subacute phase of wound healing reduces hypertrophic scar formation. Wound Repair Regen 24:644–656